Characterization of Viscoelastic Properties of Solid Biomaterials (Design and Prototype)

BY

Natavee Srifah 63011196
Orrakod Mujchachum 63011228

A PROJECT SUBMITTED IN PARTIAL FULFILLMENT OF THE REQUIREMENTS FOR THE DEGREE OF BACHELOR OF ENGINEERING IN BIOMEDICAL ENGINEERING
KING MONGKUT'S INSTITUTE OF TECHNOLOGY LADKRABANG
ACADEMIC YEAR 2023

SCHOOL OF ENGINEERING

KING MONGKUT'S INSTITUTE OF TECHNOLOGY LADKRABANG

PROJECT CERTIFICATE

Project Title	Characterization of Viscoelastic Properties of Solid Biomaterials (Design and Prototype).
Student Name	Miss Natavee Srifah Student ID. 63011196 Miss Orrakod Mujchachum Student ID. 63011228
Degree	Bachelor of Engineering in Biomedical Engineering
Project Advisor	Signed: _____ (Asst. Prof. Dr. Kasama Srirussamee)
Committee	Signed: _____ (Assoc. Prof. Dr. Matthew Paul Gleeson)
Committee	Signed: _____ (Asst. Prof. Dr. Jamie Alexander O'Reilly)
Committee	Signed: _____ (Asst. Prof. Dr. Pimkhuan Hannata-an)
Committee	Signed: _____ (Dr. May Phu Paing)
Head of Department	Signed: _____ (Assoc. Prof. Dr. Sarinporn Visitsattapongse)

Project Title	Characterization of Viscoelastic Properties of Solid Biomaterials (Design and Prototype).
Student Name	Miss Natavee Srifah
	Miss Orrakod Mujchachum
Degree	Bachelor of Engineering in Biomedical Engineering
Project Advisor	Asst. Prof. Dr. Kasama Srirussamee
Academic Years	2023

ABSTRACT

Viscoelasticity is a fundamental property of materials that has important roles in biomaterials and is involved in some of the medical device failures. In this study, a viscoelastic testing device was designed and fabricated to characterize the behavior of solid biomaterials, of which a commercial eraser was used for pilot test of load cell components. We conducted a relaxation test following Maxwell's model to measure the stress of the eraser at three different levels of strain of 10%, 20%, and 30% using two methods. Initially, a c-clamp was employed in the first part of the project, followed by the development of a machine incorporating a mechanism for controlled movement. The results indicate that maximum stress was dependent on the level of applied strain, with the c-clamp method recording 389.399 kPa, 592.259 kPa, and 1095.702 kPa at 10%, 20%, and 30% strain, respectively. In contrast, the motor assembly method recorded 0.851 kPa, 0.224 kPa, and 2.368 kPa at the same strain levels. These results follow Hooke's law, however, the significant differences between the two methods highlight the impact of compression force application (manual and stepper motor) and the lateral shear stress induced by the rotation of the press plate. At 30% strain, an excessive amount of stress led to a reduction in stress relaxation time and material fracture. This study demonstrates that the load cell, displacement sensor, and motor mechanism components are capable of characterizing the stress relaxation behavior of materials. Future development could focus on minimizing various factors and complexities to enhance the device's potential for viscoelasticity characterization.

ACKNOWLEDGEMENTS

I would like to express my deepest appreciation to my professor, Asst. Prof. Dr. Kasama Srirussamee, who gave us the opportunity to learn more about the viscoelastic properties of solid biomaterials through this project and also for helping when we face unexpected problems. He can guide and teach us in both theoretical and practical ways with reliable knowledge. We have learned a lot of new things, not only the project methodology, but also how to handle all engineering tools, how to write a reliable thesis and how to work effectively. As well as giving encouragement and not leaving us alone. His guidance and advice have been invaluable and carried us through all the stages of doing our project.

Finally, we would like to acknowledge our parents and friends for their support and encouragement throughout the period of this project.

Natavee Srifah and Orrakod Mujchachum

TABLE OF CONTENTS

LIST OF TABLES

Tables Page

LIST OF FIGURES

CHAPTER 4 EXPERIMENTAL RESULT

LIST OF SYMBOLS/ABBREVIATIONS

Symbols/Abbreviations	Terms
E	Elastic Modulus
hr	Hours
kPa	Kilopascal
mm	Millimeter
N	Newtons
Nm	Newton Meter
ε	Strain
σ	Stress
s	Second
η	Viscosity

CHAPTER 1
INTRODUCTION

1.1 Introduction

Viscoelasticity, the time dependent deformation of materials under stress, is a basic feature that describes the mechanical behavior of fundamental property [1]. Viscoelasticity has an important role in an area of research in biomedicine, contributing to the knowledge of biology activity and the development of treatment and diagnostic strategies for a range of clinical problems [2]. For instance, viscoelasticity is essential in analyzing the dynamic loading experienced by natural cartilage or total knee replacement during high-intensity activities like downhill skiing, which can differ significantly from the controlled testing performed in a laboratory [2]. Therefore, the study of viscoelasticity has a significant impact on the development of new technologies and therapies that can enhance the quality of life for patients with various clinical problems.

Viscoelasticity is the substance's ability to demonstrate both elastic and viscous behavior while elastic material immediately returns to its original shape when the force is removed, the viscous material does not [3]. Viscoelasticity is a time-dependent property that dictates the mechanical functionality of material over time [3]. The viscoelastic properties of medical device materials are important because it can help prevent failure of device parts.

Therefore, understanding the viscoelastic properties of medical device materials is important to prevent failure of the device parts. If it is not taken into consideration during the design and selection of materials it can lead to mechanical failure [4].

This project presents a plan for study the importance of viscoelastic property and design a prototype of a simple device that is able to characterize the viscoelastic properties of solid biomaterials in vitro, based on the working principles of the current devices already available in the market [6].

1.2 Objectives of the study

- Design a prototype of a viscoelastic measurement machine.
- To evaluate the performance of the prototype.

1.3 Scope of the study

This project aims to understand the characterization of viscoelastic properties of solid biomaterials. There are two parts of our machine: designed; and assembly. The design part we study about all the mechanisms that are involved in this machine, including mathematical calculation and the assemble part we use the electronic components that we research and connect with the microcontroller to control our mechanisms. This project will focus on the characterization of the solid material's response to applied deformation compared with the

commercial machine but in laboratory scale.

1.4 Report Outline

The following contents of this report is organized as follows:

Chapter 2 presents the relevant theory and mathematical review to this research.

Chapter 3 describes the design and implementation of a viscoelastic testing machine.

Chapter 4 demonstrates the experimental result of foam eraser graph

Chapter 5 discusses the work undertaken and draws conclusions about key points of this research. Finally, suggestions that can be a particular focus to further explore this study.

CHAPTER 2
THEORY

2.1 MATHEMATICAL MODEL OF VISCOELASTIC

Viscoelasticity refers to the behavior of materials that exhibit both viscous (fluid-like) and elastic (solid-like) properties when subjected to stress or strain [6]. Viscous behavior is a measure of a fluid response to flow with time when stress is applied [7]. For example, creep is a viscous behavior in viscoelastic materials when subjected to a constant load over time. Elastic behavior or solid-like properties is an immediate deformation response of viscoelastic materials.

This means that the material will deform under a load or force but will recover its original shape when the load is removed [2]. This property is important in biomaterials because it helps to simulate the mechanical behavior of biological tissues, making them useful in a variety of medical applications such as tissue engineering and implantable devices [8].

There are two main models that derive the viscoelastic equation, both models are represented as a single spring for elasticity and a single dashpot for viscous connected in series for Maxwell's and parallel for Voigt's model [1]. The equation of spring(elasticity) and dashpot(viscous) are represented following:

Elasticity

$$\sigma = E\varepsilon \tag{1}$$

where:

σ *is the stress*

ε *is the strain*

E *is the Elastic modulus*

Viscosity

$$\sigma = \eta\left(\frac{d\varepsilon}{dt}\right) \tag{2}$$

where:

σ *is the stress*

ε *is the strain*

η *is the viscosity*

Maxwell's Model

Maxwell's Model is a linear viscoelastic model that describes the behavior of materials as an elastic spring and a viscous dashpot connected in series [9].

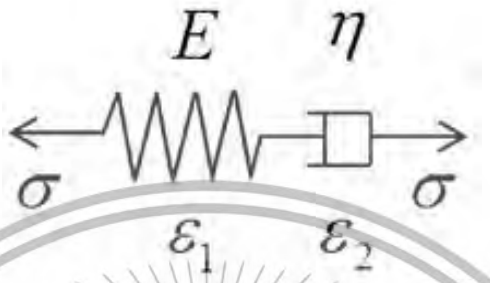

Figure 2.1 Maxwell's Model [9].

It is used to predict the creep and stress relaxation behavior of a material. The creep response is proportional to the load and time, while the stress relaxation response is proportional to the initial stress and time [10]. In this context, the derived equations of Maxwell are shown below.

First, we start with isostress and summation of strain equations.

$$\sigma_{total} = \sigma_{dashpot} = \sigma_{spring} \quad (3)$$

$$\varepsilon_{total} = \varepsilon_{dashpot} + \varepsilon_{spring} \quad (4)$$

Stress – Strain relationship, Hooke's Law state that

$$E = \frac{\sigma}{\varepsilon} \quad (5)$$

$$\sigma = E\varepsilon \quad (6)$$

Rewrite the equation as per unit of time

$$\frac{d\sigma}{dt} = E\frac{d\varepsilon}{dt} \quad (7)$$

Substitute the stress equation of dashpot and spring to the equation .

$$\frac{d\sigma}{dt} = E\left(\frac{d\varepsilon_{dashpot}}{dt} + \frac{d\varepsilon_{spring}}{dt}\right) \quad (8)$$

$$\frac{d\sigma}{dt} = E\left(\frac{\sigma}{\eta} + \frac{1}{E}\frac{d\sigma}{dt}\right) \quad (9)$$

$$\frac{1}{E}\frac{d\sigma}{dt} = \frac{\sigma}{\eta} + \frac{1}{E}\frac{d\sigma}{dt} \quad (10)$$

$$\frac{d\varepsilon}{dt} = \frac{1}{E}\frac{d\sigma}{dt} + \frac{\sigma}{\eta} \quad (11)$$

For Creep Test, stress is constant; $\sigma = \sigma_0$
Integrate equation (11) *to get an equation of creep test.*

$$\int \frac{d\varepsilon}{dt} = \frac{1}{E}\frac{d\sigma}{dt} + \frac{\sigma}{\eta} \quad (12)$$

$$\varepsilon = \frac{\sigma_o t}{\eta} + \frac{\sigma_o}{E} \quad (13)$$

For Relaxation Test, strain is constant;

$$\frac{d\varepsilon}{dt} = 0 \quad (14)$$

Substitute equation (14) *to equation* (11) *to get an equation of relaxation test.*

$$\sigma = \sigma_o e^{\left(\frac{-Et}{\eta}\right)} \quad (15)$$

Creep is the gradual deformation of a material under a constant load, and it occurs because of the viscous component of the material. In Maxwell's Model, the creep response of the material is proportional to the load and the time (Figure 2 a) [11]. Stress relaxation is the reduction in stress in a material under constant strain, and it occurs because of the elastic component of the material. Maxwell's Model has some limitations when it comes to describing the behavior of most viscoelastic materials, this model shows that the strain rate is constant when a constant stress is applied. which may be suitable for describing fluid behavior. But it does not explain the behavior of solids. In fact, many solid materials, such as polymers, do not follow this simple assumption but often exhibit more complex viscoelastic responses, where the strain rate changes over time when subjected to constant stress. Maxwell's Model is more accurate in calculating the relaxation test than the creep test [11]. In Maxwell's Model, the stress relaxation response of the material is proportional to the initial stress and the time (Figure 2 b).

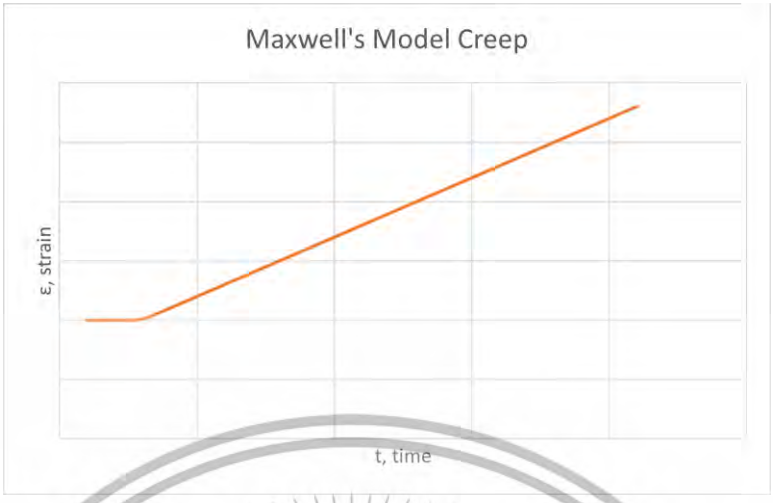

Figure 2.2 (a) Qualitative plot of Strain under constant Stress over time (Creep).

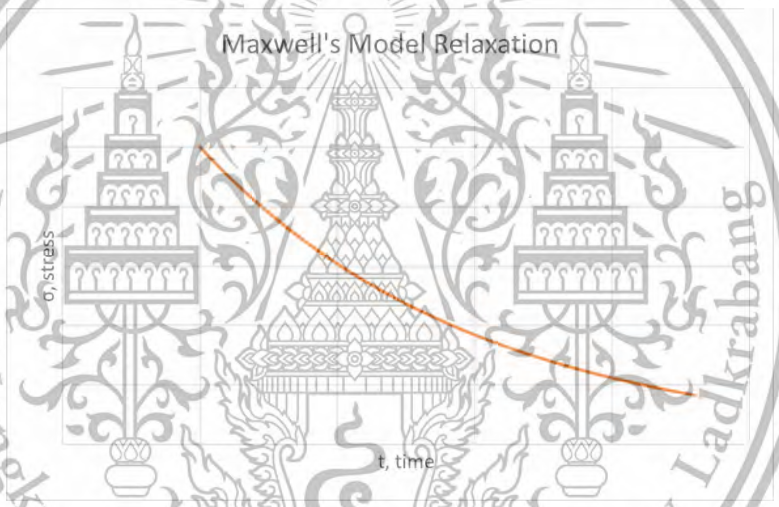

Figure 2.2 (b) Qualitative plot of Stress under constant Strainover time (Stress Relaxation).

Voigt Model

The Voigt model is a simple mathematical model of a spring and a dashpot connected in parallel [9,11]. The model represented that the material experienced both elastic and viscous responses analyzing the combination of instantaneous deformation over time.

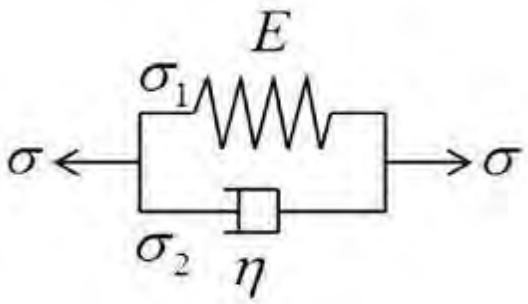

Figure 2.3 Voigt Model. [9,11]

It can be represented by the equation shown following:

$$\sigma_{total} = \sigma_{dashpot} + \sigma_{spring} \quad (14)$$

$$\varepsilon_{total} = \varepsilon_{dashpot} = \varepsilon_{spring} \quad (15)$$

Substitute the stress equation of dashpot and spring to the equation .

$$\sigma_o = \eta \frac{d\varepsilon_{dashpot}}{dt} + E\varepsilon \quad (16)$$

$$\frac{d\varepsilon}{dt} = \frac{\sigma_o}{\eta} - \frac{E\varepsilon}{\eta} \quad (17)$$

For Creep Test, stress is constant
Integrate equation (17) *to get an equation of creep test.*

$$\varepsilon = \frac{\sigma_o}{E}(1 - e^{(\frac{-Et}{\eta})}) \quad (18)$$

For Relaxation Test, strain is constant
Substitute equation (19) *to equation* (17) *to get an equation of relaxation test.*

$$\frac{d\varepsilon}{dt} = 0 \quad (19)$$

$$\sigma = E\varepsilon_o \quad (20)$$

When a force is applied, there is no instantaneous deformation due to the inability of the dashpot to change shape instantly [11]. Voigt's model is realistic when it comes to predicting the gradual decrease in strain over time when the stress remains constant (Figure 4 a.) [10]. It is especially useful in modeling the gradual deformation of materials over time, commonly referred to as creep or to input a constant stress. However, Voigt's model has limitations when it comes to capturing certain aspects of material behavior. For example, it cannot accurately predict relaxation that varies with time, and it also does not account for permanent deformation when a load is removed. This means that the Voigt model may not fully represent the way some materials behave in real-world situations. When dealing with viscoelastic materials that exhibit time-dependent relaxation (where stress gradually decreases over time under a constant strain) or materials that experience permanent deformation after a load is released, the Voigt model's predictions may fall short, which means the model is less precise in predicting the behavior of relaxation (Figure 4 b.) [12].

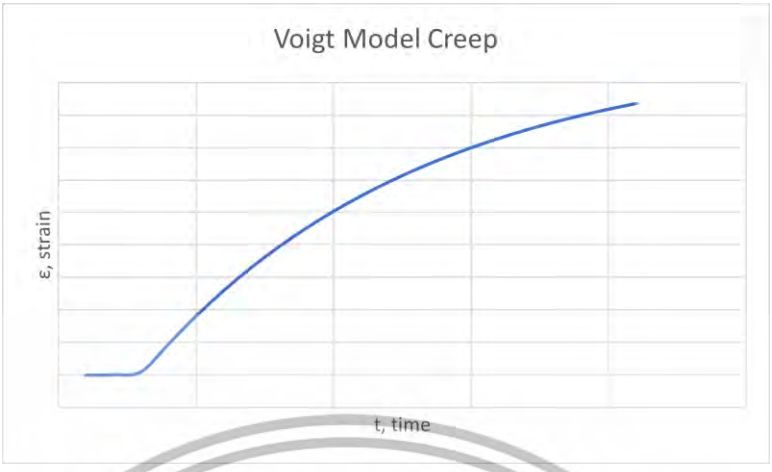

Figure 2.4 (a) Qualitative plot of Strain under constant Stress over time (Creep).

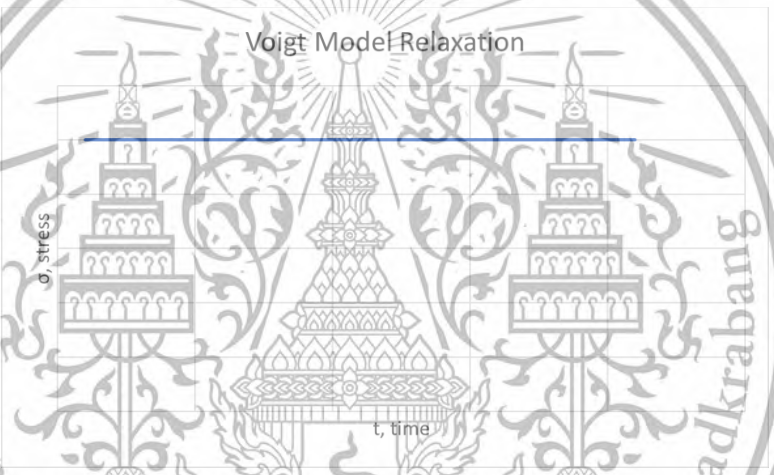

Figure 2.4 (b) Qualitative plot of Stress under constant Strain over time (Creep).

2.2 MATERIAL REVIEW

2.2.1 Force sensor

A force sensor or force transducer, that converts mechanical forces, such as weight, tension, compression, torque, strain, stress, or pressure, into an electrical output signal. This electrical signal is measurable, and convertible, and it changes proportionally as the applied force on the force sensor increases [18]. In the material review of the force sensor, we explored four components commonly used for force and pressure measurements.

Starting with the Force Sensing Resistor, it employs a change in resistance within its polymer matrix when subjected to force [19]. This provides the advantage of a wide dynamic range and cost-effectiveness. However, FSRs suffer from lack of precision, with measurement error often exceeding 10%, making them unsuitable for precise weight measurements [20]. The greater the force applied, the lower the resistance.

Figure 2.5 Force Sensing Resistor [19].

Load cells function through strain gauges, converting mechanical deformation into electrical signals. Their main advantage is high precision, making them ideal for weight measurements but the load cells can be more expensive and require precise calibration [21].

Figure 2.6 Load Cells [21].

Piezoelectric sensors rely on the piezoelectric effect to generate an electric charge under mechanical stress. Their quick response and high sensitivity are their advantages. However, these sensors are sensitive to temperature changes and may require additional circuits for signal adjustment [22].

Figure 2.7 Piezoelectric Sensors [23].

Capacitive Force Sensors measure capacitance changes between two plates when force is applied. They have high accuracy and toughness, making them suitable for various applications [24]. But, they can be expensive and can be affected by external electrical interference.

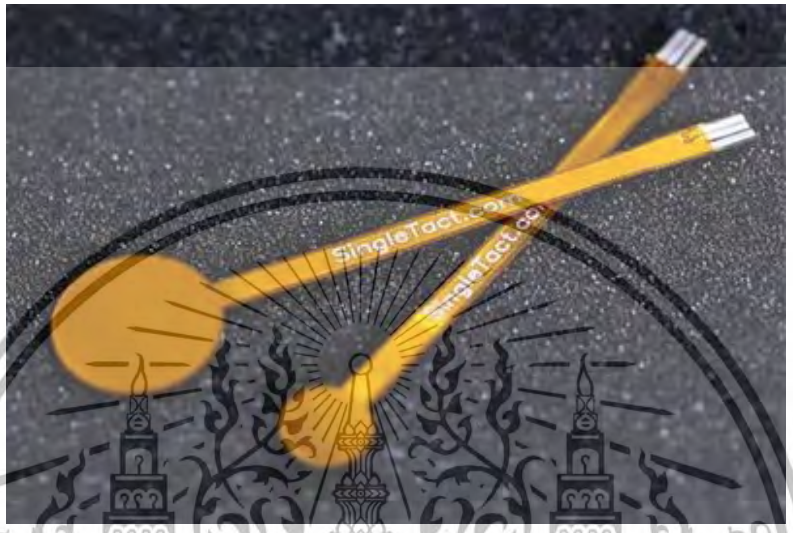

Figure 2.8 Capacitive Force Sensors [25].

Table 2.1 Force Sensor Review.

Type	**Principle**	**Advantages**	**Disadvantages**
Force Sensing Resistor [13]	The resistance of the sensor decreases inversely proportional to pressure applied to its surface.	- The price is affordable - User-friendly	- Low precision of 10%. - More different in measurement result. - It is not suitable for weighting.
Load cells [14,15]	The output is returned as a signal to the mechanical force applied to the system.	- Load cell has an accuracy of less than 0.1% of the full scale but bulky in size.	- It requires precise calibration to maintain accuracy over time.
Piezoelectric Sensor [16]	The transducer converts energy to voltage when it receives force or pressure.	- It has an excellent frequency response.	- It can be used only for dynamic measurement. - Requires additional circuit for adjustment.

Capacitive Force Sensor [17]	It measures force by detecting changes in capacitance.	- It is simple to connect to a microcontroller. - It has a great resolution.	- It is overly sensitive to changes in the environment.

2.2.2 DISPLACEMENT SENSOR

Five displacement sensors are chosen to review as components in this project. This review intends to provide valuable insights into the selection of the most suitable displacement sensor for our project's specific requirements to calculate deformation of a material.

First, a diffuse displacement sensor. It uses a light source to project light onto an object and then reflected onto a receiving lens through an electrically connected cable. This sensor is capable of measuring distances up to 250 mm with high accuracy for an opaque material but it is very expensive with a lot of accessories.

Figure 2.9 Diffuse Displacement Sensor [31].

Next are proximity sensors. It uses magnetic fields to detect objects that have a range of 15-20 mm. The subject tested does not require a magnetic object. However, it is too expensive for this project.

Figure 2.10 Proximity sensors [27].

Then there are ultrasonic sensors that use sound waves and echoes of an object and convert a speed of sound into distance. However, they are more expensive compared to other types of sensors.

Figure 2.11 Ultrasonic Sensor [32].

Another type is a laser ranging and gesture, GY VL53L0X. It uses infrared light to measure that work up to 2 meters maximum with discrepancy of 1 mm and the ability to combine with Arduino and other accessories. However, outdoor usage can be influenced by environmental factors.

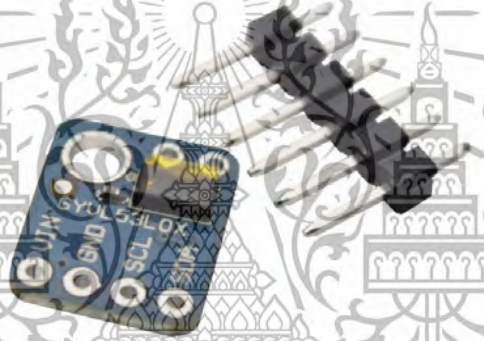

Figure 2.12 Laser ranging and gesture Sensor,GY VL53L0X, [29].

Lastly, a laser ranging sensor module. It uses a laser or infrared light source to measure the time it takes for the light to bounce off an object and return to the sensor similar to the GY VL53L0X but, with a range of 0-50 mm. It can be used in various applications, such as automated systems and touchless interfaces.

Figure 2.13 TOFO 050C VL6180, Laser ranging and gesture Sensor [30].

Table 2.2 Displacement sensor review.

Type	Principle	Advantages	Disadvantages
Diffuse Displacement Sensor [26]	It uses a light source to emit to the object and reflect to the receiving lens through electrical cable and calculated by the time it takes to travel to the object and back.	- It can measure distance up to 250 mm. - High accuracy for opaque material.	- It is very expensive with a lot of accessories that might further add to the overall cost.
Proximity Sensor [27]	Use magnetic fields for detecting magnetic objects within the range of 15-20 mm.	- The subject to be tested does not require a magnetic object. - It can be used in a variety of applications and environments.	- It is relatively expensive.
GY VL53L0X (Laser ranging and Gesture Sensor) [28]	Use infrared to measure the gesture with a maximum range of 2 meters with discrepancy of 1 mm.	- It is capable of various applications due to a good range. - Can be coded by using Arduino and can be combined with other accessories.	- It can be affected by environmental conditions when used outdoors.
Ultrasonic Sensor [29]	Use ultrasound and echoes of an object and convert a speed of sound into distance.	- It works well in various environments and is useful for non-contact measurement.	- It was relatively expensive, compared with other types.
VL6180 Laser Ranging Sensor [30]	Use a laser source to measure the time of the light to return and convert to distance.	- Compact in size and suitable for short range distance.	- It cannot be used with oblique materials due to laser ranging.

2.2.3 COMPRESSION MACHINE MECHANISM

We searched for important components such as a microcontroller, a motor that drives mechanically moved objects, a lead screw that cooperates with a motor to drive the object, and torque.

A. Arduino Uno

Arduino is an open-source microcontroller to use hardware and software components for programming and building circuit boards [33]. It consist of 14 digital input/output pins, 6 analog inputs, a USB connection, a power jack, and a reset button [34].

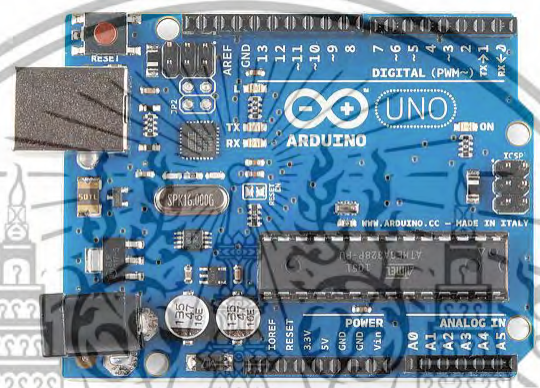

Figure 2.14 Arduino Uno [35].

B. Motor driver

A motor driver, such as the L298N, serves as a component linking motors and control circuits. This is particularly important because motors typically demand high current levels, while control circuits operate using low-current signals [36]. A motor driver like the L298N transforms a low-current control signal into a higher-current signal, allowing it to power and control the connected motor.

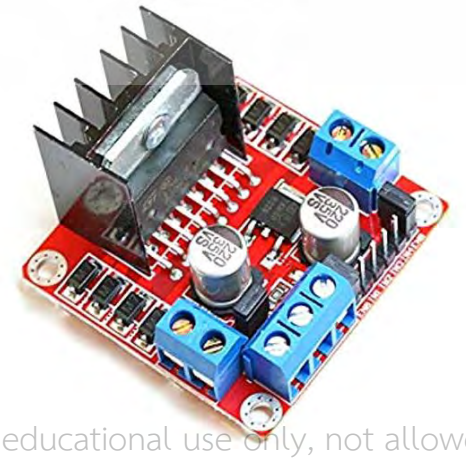

Figure 2.15 L298N Motor Driver [37].

C. Motor Review

There are five mechanisms being considered for their ability to compress materials. We review various mechanisms essential to our project. These mechanisms play a crucial role in shaping the functionality and performance of our system. Each mechanism offers a unique set of advantages and limitations, making it important to carefully consider the specific requirements of our project. By evaluating these mechanisms, we aim to make informed decisions that will contribute to the project's success.

First, stepper motor, a motor that converts electrical power into mechanical power that requires a lead screw to control. It can be used with microcontrollers and simple motion setups. Stepper motors provide precise position control over position and speed without requiring feedback that is useful for maintaining compression accuracy [38]. Additionally, it has high torque at low speed. Moreover, it is easy to use, requiring only easy control circuits or programming and cost-effective.

Figure 2.16 Nema 17 Stepper Motor 17HS4401S [43].

Second, a DC gear motor is a combination of a motor and gearbox to reduce the speed but increase the torque output, that uses direct current to drive the motor's rotation. These motors are easy to use, cost-effective, and provide various ranges of speeds and torques [44].

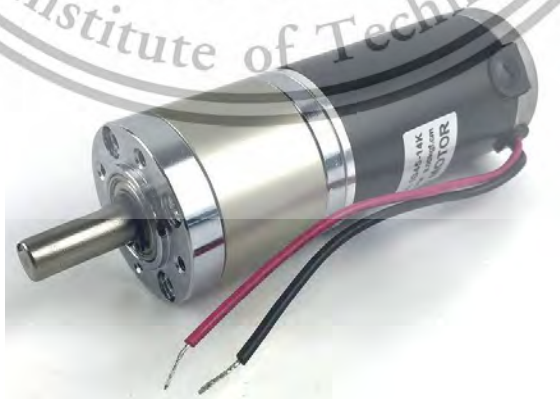

Figure 2.17 DC gear motors [45].

Servo Motors use feedback mechanisms for accurate angular control. Their high precision, speed, and multipurpose make them suitable for tasks requiring precise control. However, they can be more complex and expensive compared to other motors [46].

Figure 2.18 Servo Motors [46].

The fourth mechanism is Linear Actuator, an electric motor that converts a rational motion into linear motion. Include a lifting column and a lead screw as a frame. It allows a smooth motion control system and pushing and requires feedback [47].

Figure 2.19 Linear Actuator [48].

Hydraulics use fluid under pressure to generate mechanical motion. They provide a lot of power density suitable for heavy-duty applications. Yet, designing can be complex, and leakage is a potential issue, and require maintenance [49].

Figure 2.20 Hydraulic Compression Machine [49].

D. Push button 2-Pin

Push buttons or switches are digital input devices commonly used with Arduino microcontrollers [50]. They are fundamental for creating user interfaces and controlling various

functions in Arduino projects as coded.

Figure 2.21 2-Pin Button [51].

Table 2.3 Mechanism Review.

Type	**Principle**	**Advantages**	**Disadvantages**
Nema 17 Stepper Motor (17HS4401 S) [38]	Convert electrical power to mechanical. It is typically 1.8 step angle and 200 revolution per angle.	- It provides impressive torque at low speeds. - Great for positioning motion with high efficiency. - It is easy to use, requiring only easy control circuits or programming. - Cost-effective	- Low acceleration. - Require a base, a slider, and a lead screw.
DC gear motor [39]	The DC motor is simple, speed can be adjusted by varying the input supply voltage. Required a lead screw.	- Higher speed range and maximum load.	- It is not efficient in controlling and positioning.
Servo Motor [40]	Uses a rotary of linear actuators. Mostly used for remote controls.	- It works better for complex systems that require feedback. - It can rapidly respond to control commands, making them suitable for real-time applications.	- More complex to set up and control due to feedback systems and controllers.

Linear Actuator [41]	It converts rotational motion to linear motion. Require a lead screw.	- It can be used with Arduino. - Provide smooth operations	- It is relatively expensive.
Hydraulic [42]	It is commonly used for compression and mostly used for high force such as press and lifts.	- It has a precise and controlled motion. - Great power for heavy-duty applications.	- It cannot be controlled by a microcontroller. - It is relatively expensive.

E. Lead Screw

Lead screw is a mechanical component that is commonly used to convert rotational motion into linear motion [52]. The motion of a lead screw relies on the screw shaft and the nut threads. There are two key components which are screw shaft and a nut. As the screw shaft rotates, the nut moves along a threaded path which results in linear movement. It can produce large forces by applying small moments [53].

The pitch is the distance between screw threads and lead is the linear distance travel per one revolution or 360 degrees [54]. There are 4 major types of thread start. single lead, double lead, triple lead and quad lead. This can be determined by defining the start point, end point, and the shape of the lead start [55].

Figure 2.22 Type of lead [56].

There are three types of thread profile classified by geometry; ACME thread, buttress thread, Square thread. Each type of profile has a different property and mechanism of the use of it.

The ACME thread is a trapezoid-shaped thread. It consists of strength at the base making it stronger and higher clamping speed. It has a good load capacity but less efficiency due to the friction in high speed and precision application [54].

The buttress thread is a triangular thread that has a high thread strength in one direction. It is an asymmetrical thread profile that has a wider base of thread used to transmit power. One side of steep angle and one side of shallower angle. However, it has a limited availability due to the direction and the friction it encountered [56].

The square thread has a symmetric square-shaped thread with a low friction thread due to its thread angle and precision positioning with well-suited speed. Yet, it has a limited load capacity and complex manufacturing compared to others [57].

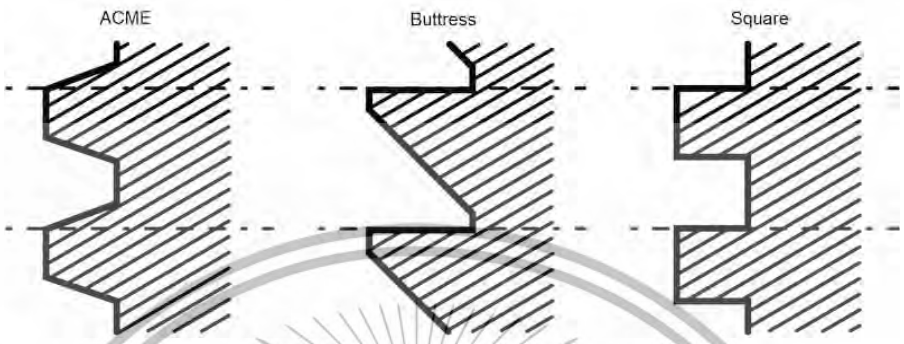

Figure 2.23 Types of lead screw [53].

Table 2.4 Types of thread profile.

Type	**Principle**	**Advantages**	**Disadvantages**
ACME Thread [57].	- Trapezoid thread or a steep thread - 290 degrees thread angle - designed for rotary motion to linear	- good load capacity	- less efficiency due to friction.
Buttress Thread [57].	- asymmetrical thread profile transmit power in one direction - consist of steep angle and a shallower angle	- high load capacity and power - great efficiency.	- limited availability - high friction
Square Thread [57].	- symmetric thread profile - matching with square screw to create a linear motion	- high efficiency - precision positioning - well-suited of low speed	- complex manufacturing - limited load capacity

F. Torque

Torque is a rotating force exerted or rotating something to produce the rotary motion in the direction we want to make an object tight, loosen, or rotate to the position. For example, opening the door knobs or caps of bottles, or tightening nuts or wheels to change a tire [58]. It could be observed that when tightening car wheel nuts, using a short wrench handle requires higher force than the longer handle, which requires less exerted force [59].

Therefore, torque is determined by multiplying the force exerted to an object by its distance from the rotational axis. The SI unit of torque is Newton-meter(Nm).

Torque

$$\tau = Fd \tag{21}$$

where:

τ *is torque* (Nm)

F *is the perpendicular component of the applied force* (N)

d *is the radial distance* from the rotational axis (m)

CHAPTER 3
METHODOLOGY

The first section of this chapter describes the project's mathematical model design and calculations. Then, the second section outlines the manufacturing components, which include the testing of the force sensor using a c-clamp, the assembly procedure of force sensor and displacement sensor, the materials used for testing, and coding that describes how electronic components are being used in the system.

3.1. MATHEMATICAL MODEL OF VISCOELASTIC

3.1.1. Mechanism Design and Calculations

Our machine design includes the principle of mechanical optimization by precisely designing a system that virtually eliminates significant factors such as the moment. This is achieved by reducing the distance involved and directly applying force to the materials.

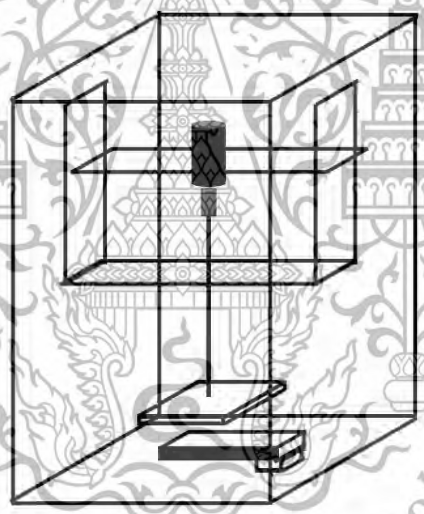

Figure 3.1 Platform design.

Major considerations of our mechanical design are the friction, moment, and corresponding reaction of the moment [60]. To reduce the effects of the moment, it is necessary to minimize the distance between the moment's center or the rotating point where the reaction force might occur. So, we ensure that the point of compression onto the materials aligns with the rotating point. Also, modify the structure by drilling into the side of the box that we used as a platform and add two platforms: one for the motor, allowing free movement, and another for the screw shaft, which remains fixed in place.

The failure force of the eraser, as determined in the first phase of the project, results in thirty percent of the materials, which is a crucial parameter for selecting the most suitable motor. It is essential to consider that the maximum load the eraser can withstand is 115 newtons. The experiment is shown in the following part. To calculate the optimal motor for our system, we take into account the eraser's load bearing capacity and additional specifications, such as diameter of the lead screw, which is 8 millimeters with a thread pitch of 2 millimeters.

Mathematical Square-threaded screws calculations

A screw with square threads is a mechanical device designed to generate a large axial force by applying a relatively small torque about the screw's axis. The view can be visualized as a rectangular bar wrapping around a cylindrical shaft, as illustrated below.

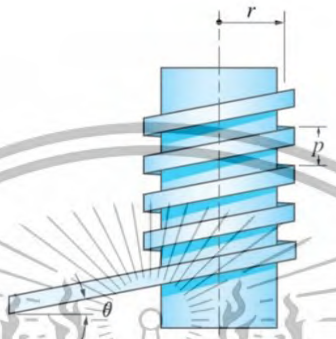

Figure 3.2 Square-threaded screw [59].

The rectangular bar is turned or rotated along the cylindrical shaft and surface engaged with the corresponding threads. This translates rotational motion into linear motion. This mechanism suits high power generated movement.

Screw are related by

$$p = 2\pi r \tan\theta \tag{22}$$

where :

θ *is the lead angle* (m)

p *is the pitch* (m)

r *is the mean radius* $(degree)$

Find the angle by substitute the value we have

$$p = 2\pi r \tan\theta \tag{23}$$

$$0.002\,m = 2\pi\,(0.004\,m)\,\tan\theta \tag{24}$$

$$\theta = \arctan\frac{(0.002\,m)}{2\pi(0.004\,m)} \tag{25}$$

$$\theta = 4.5499°$$

The screw will be utilized on a screw shaft similar to the (figure 25.) In this context, we can recall Coulomb's friction theory which states that it is independent of the contact area and assumes the contact area to be very small.

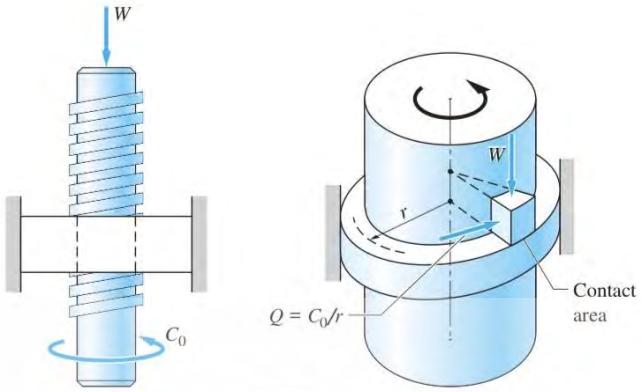

Figure 3.3 Contact area of screw [59].

The entire weight is carried by the contact area and the horizontal force:

$$Q = \frac{C_o}{r} \tag{26}$$

where :

Q *is the horizontal force* (N)

C_o *is the torque* (Nm)

r *is the radius* (m)

It can be seen that the block is being pushed by the horizontal force and can be assume that:

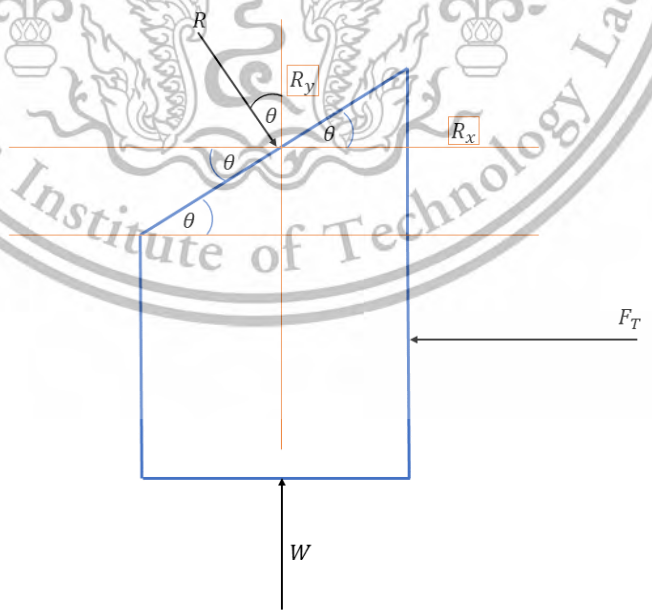

Figure 3.4 Force Vector.

The equilibrium of the block are

$$\Sigma F_y = 0; \qquad -R\cos\theta + W = 0 \qquad (27)$$
$$R\cos\theta = W$$

$$\Sigma F_x = 0; \qquad R\sin\theta - F_y = 0\,; \qquad (28)$$
$$R\sin\theta = F_T$$

$where:$

$W\ is\ the\ weight\ (N)$

$R\ is\ the\ normal\ (N)$

$F_T\ is\ the\ force\ of\ torque\ (N)$

$F_y\ is\ the\ vertical\ force\ (N)$

$F_x\ is\ the\ horizontal\ force\ (N)$

$Find\ R$

$$R\cos\theta = W \qquad (29)$$
$$R\cos(4.5499) = 115\ N$$
$$R = \frac{115\ N}{\cos(4.5499)}$$
$$R = 115.3715$$

$Find\ F_T$

$$R\sin\theta = F_T \qquad (30)$$
$$(115.3715\ N)\sin(4.5499) = F_T$$
$$9.152\ N = F_T$$

$Find\ Torque$

$$Q = \frac{C_O}{r} \qquad (31)$$
$$9.152\ N = \frac{C_O}{0.004\ m}$$
$$C_O = 0.036608\ Nm$$

Based on the calculations, the motor selected for our machine application should possess a torque capability greater than 0.036608 Nm in order to meet the machine's requirement for maximum force. This will ensure that the motor can effectively generate the power required for the machine.

3.2. MANUFACTURE PART

Following the completion of the design part of our machine, we move forward to the manufacturer part. We continue building the machine's frame and assembling all the needed hardware onto the frame. This section will describe the manufacturing process of c-clamp, machine's frame, platforms, and electronics components.

3.2.1. C-CLAMP

In this first experiment, we conducted force sensor testing using a c-clamp to test whether it is suitable to determine viscoelastic characteristics. The c-clamp used to clamp the load cell to a table to secure and apply force to the material that was put on the other side that floated in the air (Figure 28.). A longer screw is turned to compressed 10%, 20%, 30% of material's thickness to load force to the testing material and we can adjust the distance between the upper side of the load cell and lower side of the c-clamp by vernier caliper.

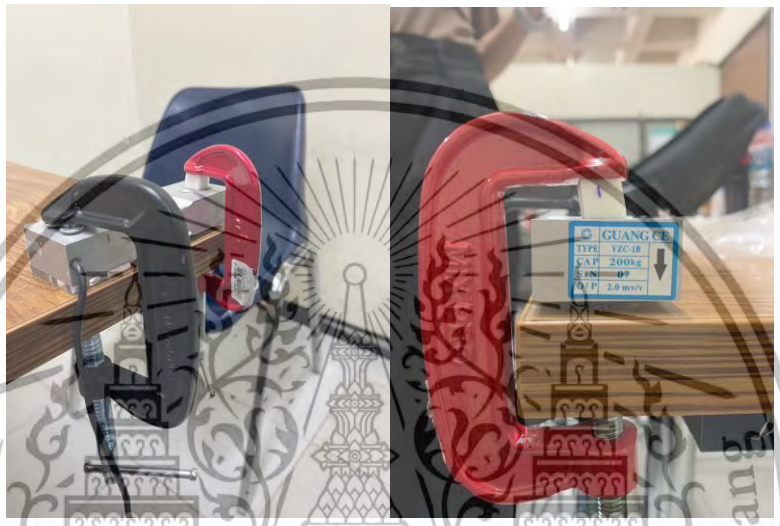

Figure 3.5 C-clamp Assemble.

3.2.2. MACHINE'S FRAME

We have chosen a wooden box as our machine's frame for the second experiment because it is easy to drill and convenient to install the components. We drilled holes in the wooden frame to install the load cell and create a route along the side of the box for the platforms. The first platform is designed to house the stepper motor, allowing for free movement. And another platform for the ball screw nuts, which will remain fixed in place.

Figure 3.6 Route for platforms and Drilling for inserting the load cell.

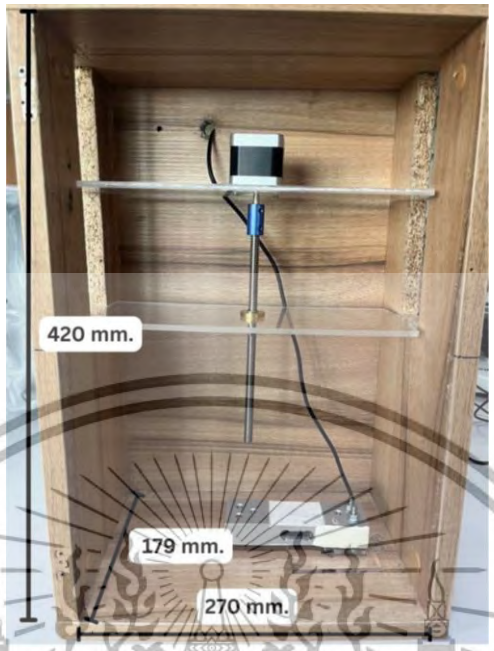

Figure 3.7 Size of wooden box.

3.2.3. FREE PLATFORM

We have selected an acrylic sheet as our platforms due to its strength, which does not bend as the stepper motor is placed on it. This platform will move along the side of the box to prevent it from rotating itself while the stepper motor is working.

Figure 3.8 Free platform.

3.2.4. FIXED PLATFORM

Acrylic sheet is convenient to customize and drill to install the ball screw nut that allows the screw shaft to move pass, which will remain fixed in place as a strong foundation.

Figure 3.9 Fixed platform.

3.2.5. ASSEMBLE ALL MACHINE FRAME COMPONENTS.

We assembled all the components inside the wooden box by inserting the fixed platform and gluing it to the end of the wooden box platway. Next, we carefully screw the leadscrew onto the screw shaft of the fixed platform and insert the free platform with the motor. Lastly, insert a load cell to the bottom of the box.

Figure 3.10 Assemble all the hardware components.

3.3. ASSEMBLY ELECTRONICS PART

3.3.1. STRAIN GAUGE LOAD CELL

A load cell is an electromechanical transducer that is designed for converting applied tensile force, compressive force, or pressure into an electrical output signal proportional to the magnitude of the input.

The strain gauge elements of a load cell are often arranged in a Wheatstone bridge configuration. Load cells are widely used in industrial and commercial projects to measure force and weight. We have used a load cell with a maximum capacity of 200 kg. then placed one side of the load cell on the acrylic plate and fixed it in position by tapping screw on the frame layered with acrylic plate.

3.3.2. HX 711

The Load cell generates electrical signals in millivolts which are too low to use directly, therefore, an amplifier called HX711 is required to increase their strength. The HX711 module amplifies the weak electrical output of Load cells and converts it into a digital signal that can be fed into the Arduino.

We connected the HX711 with the Load cell using four wires. Below are the connection details and diagram (Figure 33.) [15].

Red Wire of Load Cell is connected to E+ of HX711.

Black Wire is Load Cell connected to E- of HX711.

White Wire is Load Cell connected to A- of HX711.

Green Wire is Load Cell connected to A+ of HX711.

3.3.3. ARDUINO UNO

Arduino is a microcontroller platform that can be programmed to control the application of forces and measure the resulting electrical signals in viscoelastic properties testing. The Arduino can also display the deformation data in real-time and plot as a graph. This allows the detailed analysis of the material's viscoelastic properties, including creep and stress relaxation over time.

We connected the HX711 amplifier with the Arduino. The Arduino is programmed to apply a controlled force to the upper of the one side of the load cell that floats in the air and measure the corresponding electrical signals from the load cell. Below is the connection detail and diagram (Figure 33.) [15].

VCC of HX711 is connected to 5V of Arduino Uno

GND of HX711 is connected to GND of Arduino Uno

SCK of HX711 is connected to A2 of Arduino Uno

DOUT of HX711 is connected to A3 of Arduino Uno

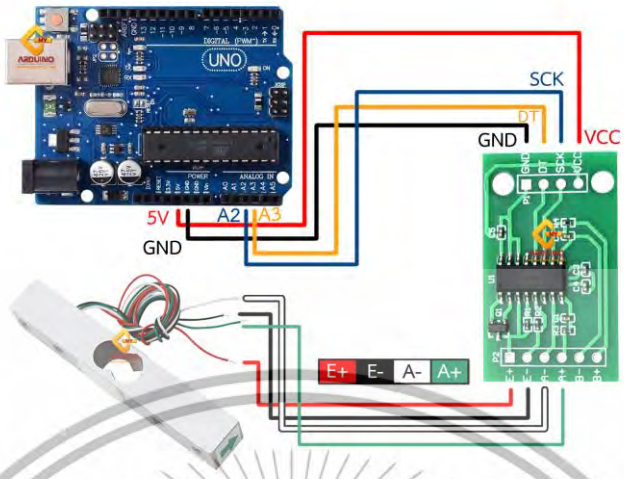

Figure 3.11 Circuit Diagram of Strain Gauge Load cell with HX711 and Aruduino[61].

3.3.4. STEPPING MOTOR

A stepper motor converts electrical power into mechanical power that requires a lead screw to control. It will be connected to the screw to create a compression by a coupling to generate a compression mechanism. A screw will be compressed to 10%, 20%, 30% of material's thickness to load force to the testing material and we can adjust the distance between the upper side of the load cell and lower side using a sensor. We connected the stepping motor and the L298N motor driver to generate the control.

A+ of Stepper motor is connected to the OUT1 of L298N

A- of Stepper motor is connected to the OUT2 of L298N

B+ of Stepper motor is connected to the OUT3 of L298N

A- of Stepper motor is connected to the OUT4 of L298N

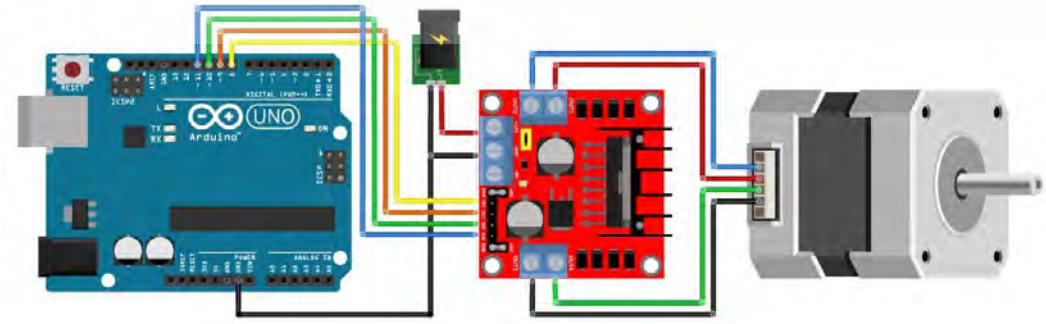

Figure 3.12 Motor and Driver assembly [61].

IN1 of L298N is connected to 8th digital pin of Arduino

IN2 of L298N is connected to 9th digital pin of Arduino

IN3 of L298N is connected to 10th digital pin of Arduino

IN4 of L298N is connected to 11th digital pin of Arduino

+12V of L298N is connected to 12V DC function generator

GND1 of L298N is connected to 12V DC function generator

GND2 of L298N is connected to the GND pin of Arduino

3.3.5. DISPLACEMENT SENSOR

A displacement sensor is a device for measuring the distance between two points by using laser ranging technology. In this study, we used the sensor to measure the compression distance of the material by attaching it near the compression platform on the box, allowing us to monitor the displacement as the material is pressed.

VCC of VL6180X is connected to the 5V pin of Arduino

GND of VL6180X is connected to the GND pin of Arduino

SDA of VL6180X is connected to the A4 pin of Arduino

SCL of VL6180X is connected to the A5 pin of Arduino

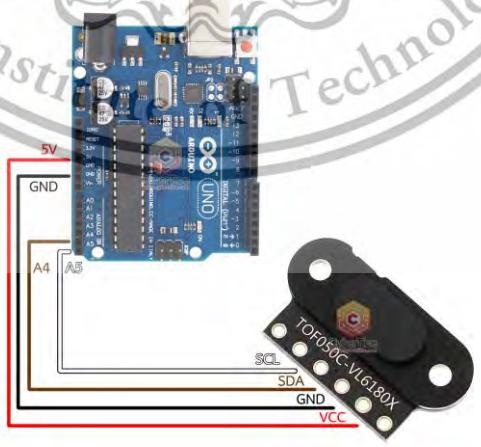

Figure 3.13 VL6180X Laser ranging assembly [62].

3.3.6. ASSEMBLE PART

The Arduino connects to all of the machine's electronics components, including the motor, load cell, displacement sensor and button. This means that all of the components are wired to the Arduino. To prevent wiring confusion, we assembled all the electronic components

inside the box, placing the driver and Arduino in the outer space of the frame. Additionally, the displacement laser ranging sensor is situated in a separate box to accurately measure the distances.

Figure 3.14 Machine Assemble.

3.4. MATERIAL PART

3.4.1. FOAM ERASER

We used a foam eraser as our testing material because the foam erasers are viscoelastic materials [63]. We cut the eraser into dimensions as follows (Table 3.1, 3.2, 3.3).

Table 3.1 Dimension of the test material of the c-clamp.

	Length (mm)	Width (mm)	Height (mm)
10% (1.26 mm)	10.80	11.50	12.65
20% (2.52 mm)	10.94	9.16	12.61
30% (3.81 mm)	9.78	10.72	12.69

Table 3.2 Dimension of the test material of the assembly machine

	Length (mm)	Width (mm)	Height (mm)
10% (1.01 mm)	9.80	12.30	10.10
20%	10.20	12.30	9.90

(1.98 mm)			
30% (2.97 mm)	10.30	12.20	9.90

Table 3.3 Dimension of the test material of the commercial machine.

(Commercial testing)	Length (mm)	Width (mm)	Height (mm)
10% (1.25)	10.90	12.50	9.10

3.5. CODING

We present an Arduino program that facilitates the calibration and measurement of weight through interfacing with an HX711 load cell amplifier and weight sensor. The program includes the definition of pins for HX711 data output (DOUT) and clock input (SCK) lines, which allows for accurate measurement of weight. The main objective of the program is to calibrate the weight sensor, which can be initiated through the reception of serial input commands (a, b, c). Upon receiving command 'a', the program executes the "Find Zero Factor" function, which sets the scale to zero and reads the average output to determine the zero factor. Command 'b' triggers the calibration factor, which adjusts the factor until the measured weight matches the known weight. Finally, command 'c' triggers the reading function, which displays the measured weight on the serial monitor [64]. Through the implementation of this program, we aim to enable precise weight measurements and accurate calibration for future progress of our field.

The code is designed to measure weight using a load cell and display the results through a serial monitor. Prior to measurement, the load cell is calibrated by entering a calibration factor to the code and the zero factor values to adjust the scale for the measurement code [64]. To compress the material and create data, we use a stepper motor controlled by two two-pin buttons on the breadboard. This button enables us to move the motor both clockwise and counterclockwise, allowing us to compress and unload the materials on the platform.

In addition, we aimed to create a graph of a viscoelastic model using the data acquired from the load cell. To accomplish this, the data was uploaded to Excel through Arduino. Specifically, we connect the communication port to establish a real-time serial communication data stream between the Arduino and Excel's data streamer [65]. By doing this, we were able to visualize the data as a graph and apply a viscoelastic model to analyze the data.

CHAPTER 4
EXPERIMENTAL RESULT

In the previous chapters, we describe detailed design and assembly procedure of the machine system. In this chapter, we present the results of our experimental testing, demonstrating the machine capability to characterized viscoelastic properties. This chapter begins with a focus on force sensors, first using a c-clamp and followed by assembly of the lead screw mechanism results. The results are presented graphically with a division of each part.

We tested the mechanical capability by using an eraser as a testing material due to its property of viscoelastic. The machine uses the mechanism of a lead screw with a motor to compress the materials. We conducted strain testing at levels of 10%, 20%, and 30%. The corresponding maximum stresses obtained were 0.851 kPa, 0.224 kPa, and 2.368 kPa, respectively. This shows that the force decreases over time. However, at 30% strain the testing machine fractured after starting shortly, so stress relaxation could not be observed.

4.1. FORCE SENSOR

4.1.1. Force Sensor using C-clamp

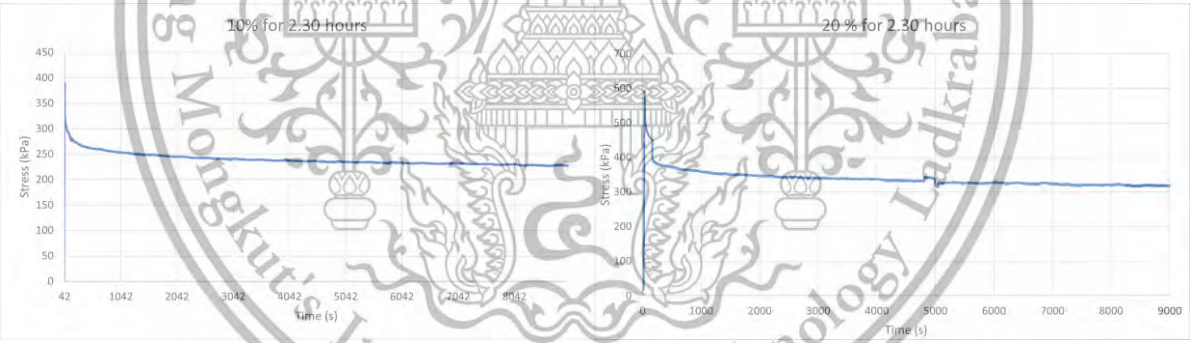

Figure 4.1 10% Strain using C-clamp.

Figure 4.2 20% Strain using C-clamp.

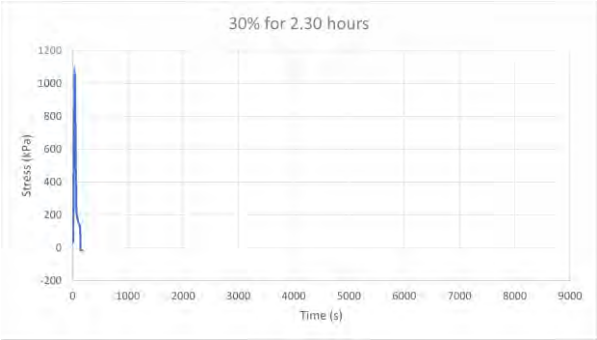

Figure 4.3 30% Strain using C-clamp.

In this experiment, we conducted strain testing at levels of 10%, 20%, and 30%. The corresponding maximum stresses obtained were 389.399 kPa, 592.259 kPa, and 1095.702 kPa, respectively (Figure 37, 38, 39.). This shows that the force decreases over time. The results have shown that maximum stress was dependent on the level of applied strain. This was due to the material properties of elastic deformation that follows Hooke's law. The force decay observed from the graph was due to stress relaxation. However, at 30% strain, too much amount of stress generated which significantly reduced the stress relaxation time and induced rapid material fracture, so stress relaxation could not be observed from this strain level (Figure 39.). It can be seen that the load cell assembled in this study could record the viscoelastic behavior of the commercial eraser. Using a c-clamp as a compressor might affect the stress obtained due to the inaccuracy of displacement measurement. Therefore, it can be further developed into the viscoelastic property characterization device by combining with the displacement control system. On the other hand, mathematical equations can also be analyzed by fitting the obtained graph.

4.1.2. Force Sensor with lead screw and motor mechanism assembly

The results have shown that maximum stress was dependent on the level of applied strain. This was due to the material properties of elastic deformation that follows Hooke's law. The force decay observed from the graph was due to stress relaxation.

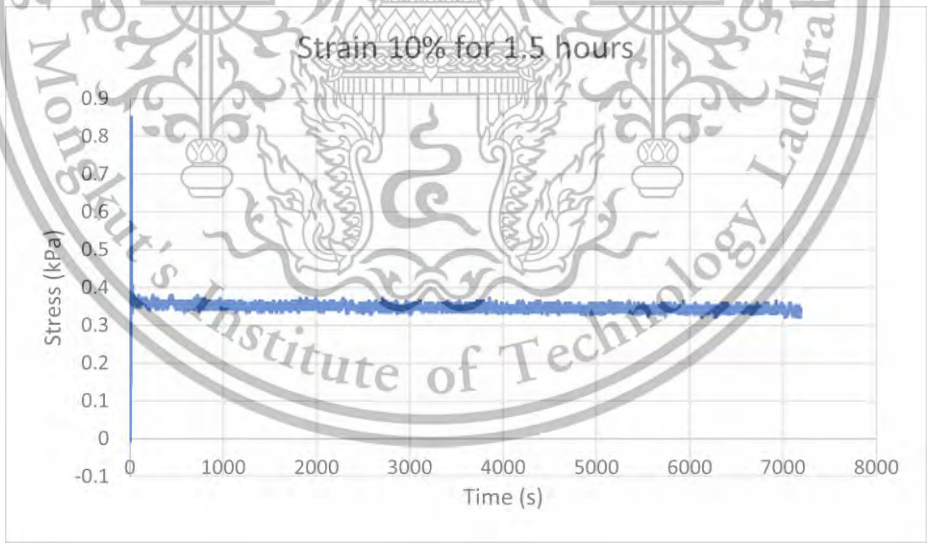

Figure 4.4 Strain 10% for 1.5 hours.

When a 10% strain is applied, the material resists the deformation, and the maximum stress reached during this resistance is 0.851 kPa. Over time, the stress will continuously decrease.

The testing described in 10% strain level demonstrates that the material exhibits resistance to applied deformation. In this section, we observed the maximum stress reaching 0.851 kPa, specifying the material's capacity to withstand moderate strain. Over time, the stress will continuously decrease, characteristic of stress relaxation behavior. When

compared with the first experiment of our project this maximum stress is higher that might be because of lead screw accuracy and displacement sensor limitations. Lead screw is one significant factor to consider in accuracy. In our machine, one full revolution of the leadscrew compresses the materials by approximately 4 millimeters. However, we must acknowledge that our displacement may not be capable of accurately measuring the distance traveled with absolute precision. The difference in measurement accuracy could lead to variations of stress values. Another possible factor that may limit accuracy is the force applied during the compression process by stepper motor. The rotation of the press plate that is connected to the lead screw introduces shear stress to the materials, meaning the force that we applied tries to shear off the material, causing it to deform laterally. These complexities in the stress distribution within the material can result in differences of recorded stress value compared to the one obtained in the lab, where it can be controlled. All of the factors mentioned above could result in distortions in stress relaxation graphs generated from our measurements. These distortions may cause fluctuations in the data making it difficult to draw direct comparisons between our results from the lab. However, the result of this level shows the characteristic of the material graph similarly to the theoretical graph.

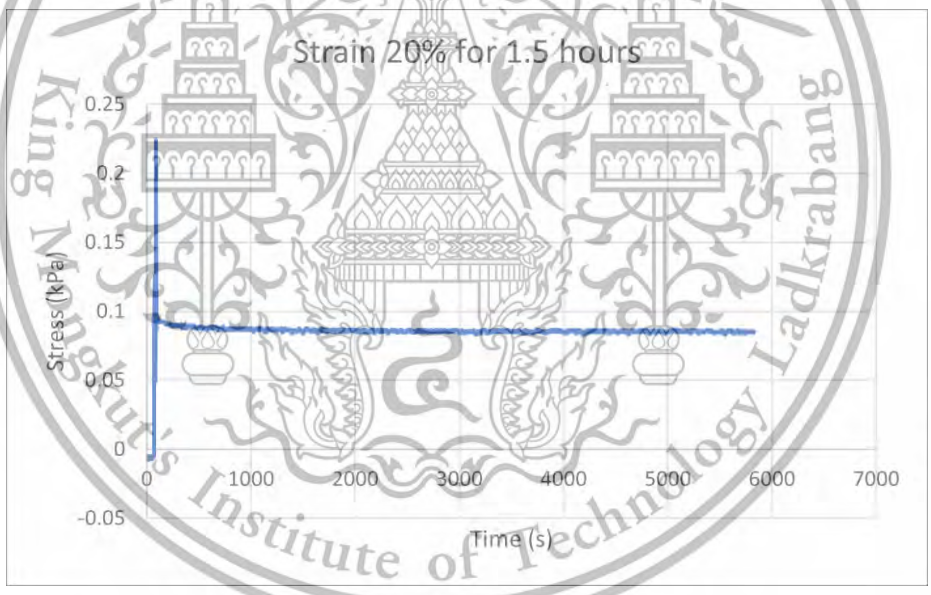

Figure 4.5 Strain 20% for 1.5 hours

When a 20% strain is applied, the material resists the deformation, and the maximum stress reaches higher than 10% strain during this resistance which is 0.224 kPa. Over time, the stress will continuously decrease.

The testing described in 20% strain level demonstrates that the material exhibits resistance to deformation, and observed the maximum stress reaching 0.224 kPa higher than 10% strain because when the material is subjected to a larger deformation, it resists more strongly and the material will show up the resist more. When compared with the first experiment of our project this maximum stress is much higher that might be due to the same factors as 10% strain level. Even at this level the result of this level still shows the characteristic of the material' graph similarly to the theoretical graph.

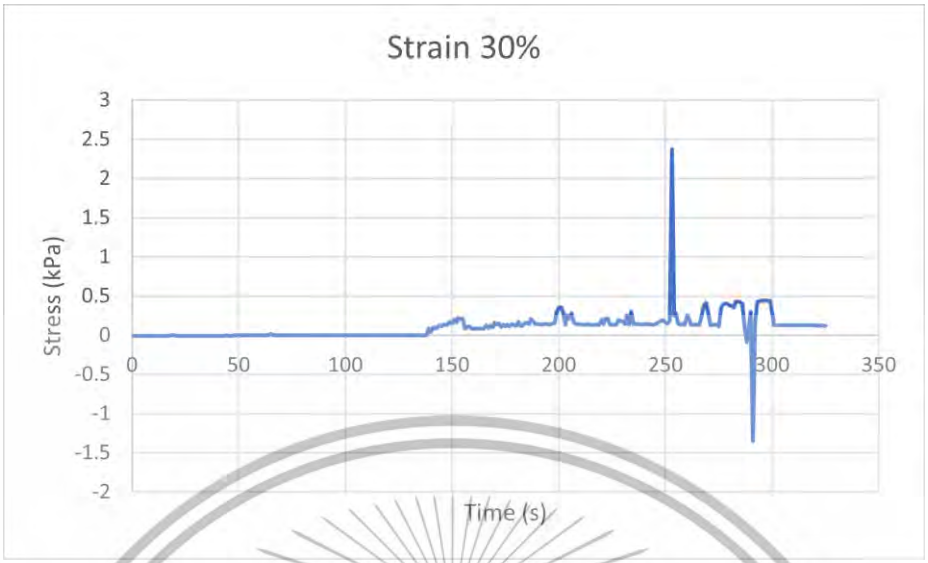

Figure 4.6 Strain 30%

When a 30% strain is applied, the material can not resist the deformation that leads the materials to undergo fracture (maximum stress = 2.368 kPa).

At the 30% strain level demonstrates that the material cannot resist the deformation that leads the materials to undergo fracture (maximum stress = 2.368 kPa). When compared with the first experiment of our project this maximum stress is much higher that might be due to the same factors as 10% and 20% strain level but the higher the strain level, the greater the shear stress on the material and that might cause the fracture of material. So at this level the result of this level cannot show the characteristic of the material' graph as similarly to the theoretical graph.

4.2. DISPLACEMENT SENSOR

The displacement sensor plays an important role in providing data of the displacement-time graph, which illustrates the material's deformation during measurement. The data of the displacement sensor combined with the load cell allows us to measure and analyze the deformation and strain trends over time. However, there may be errors to the accuracy of the displacement sensor, which we will discuss and analyze in this section.

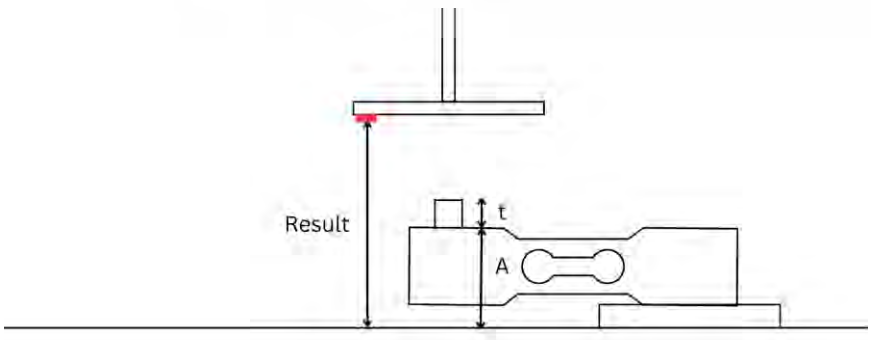

Figure 4.7 10% Displacement sensor placement.

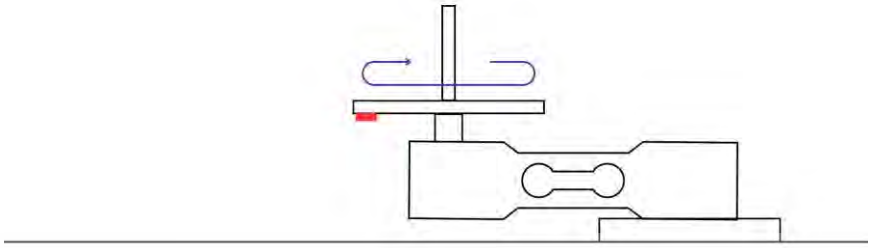

Figure 4.8 10% Displacement sensor placement when compressed.

Figure 4.9 10% Displacement-Time Curve for 1.5 hours.

The graph illustrates the measurement of deformation over time during a 10% strain. It shows the displacement sensor's ability to detect and demonstrate the displacement-time curve. In the 10% testing, the displacement sensor is positioned on the compression plate, and the data obtained involves the sensor's reading minus the distance from the load cell to the basement and the height of the material. However, the data obtained is inaccurate due to the noise. The average distance from the data is -3.636 mm while the expected distance is -1.01 mm. This experiment result as a standard deviation of $\pm$1.361.

The error observed was twice the expected value that the displacement sensor should have been measuring. Its inaccuracy might also be due to the inability to calibrate, resulting in a difference between the expected displacement and the actual measurement affected by the error. Moreover, the placement of the sensor could create fluctuations in the values, which change rapidly due to the surface it measures. This occurs as the compression plate is on rotation while the motor compresses the test material as shown in the (Figure 4.10).

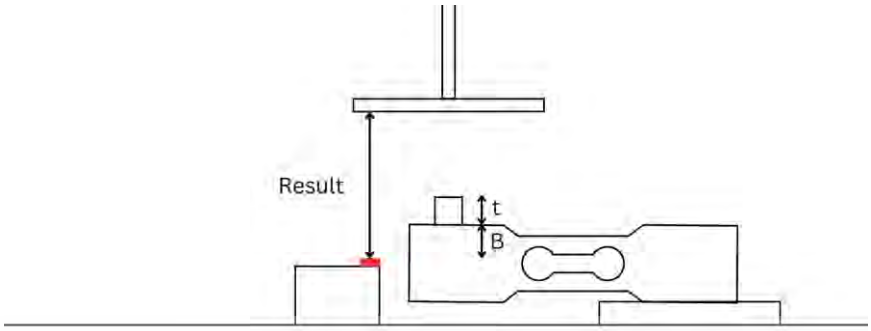

Figure 4.10 20% Displacement sensor placement.

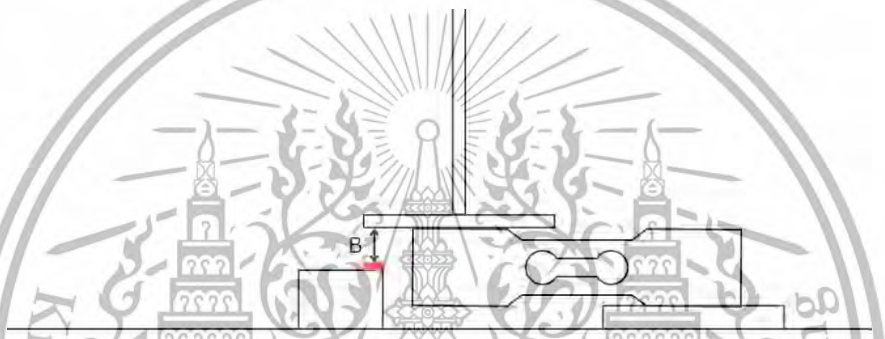

Figure 4.11 20% Displacement sensor placement when compressed.

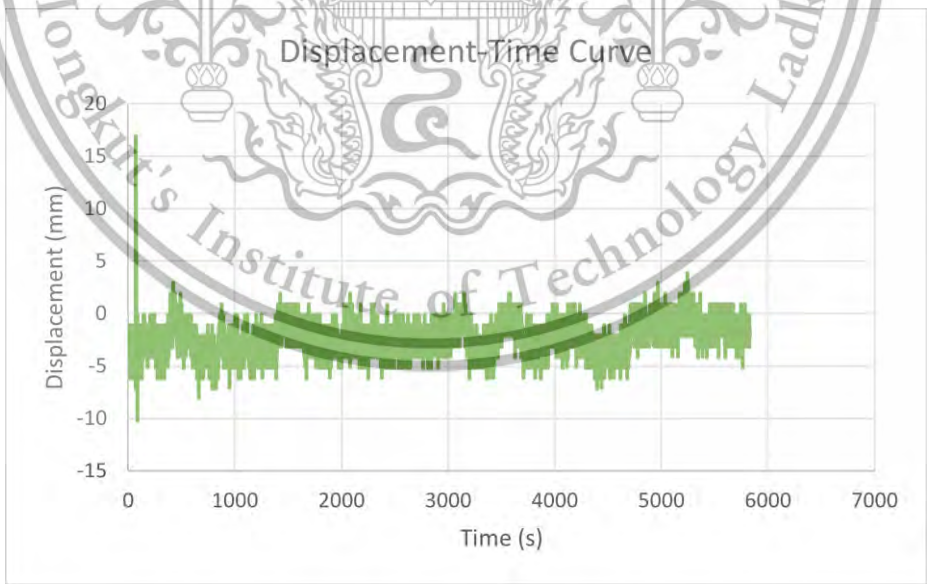

Figure 4.12 20% Displacement-Time Curve for 1.5 hours.

This graph shows the measure of deformation over time during the 20% strain is applied. The graph is able to detect the deformation which results as displacement-time curve. In the 20% testing, the displacement sensor is positioned on the additional box which remains steady still. The data obtained includes the sensor's reading subtracted from the distance of the box of sensor placement and the materials (Figure 4.10 and 4.11). The data pressed should be -

1.98 mm but the average displacement is -2.266 mm with a standard deviation of ±1.570.

The error observed in this experiment is lower than the 10% strain experiment, with an approximate difference of only 0.2 mm between the expected value and the measured value. This can be shown that the position the displacement sensor was placed is significant and can contribute to reducing measurement errors. However, even with improved positioning, there are some fluctuations in the values, which might be influenced by external factors and contribute to noises in the data.

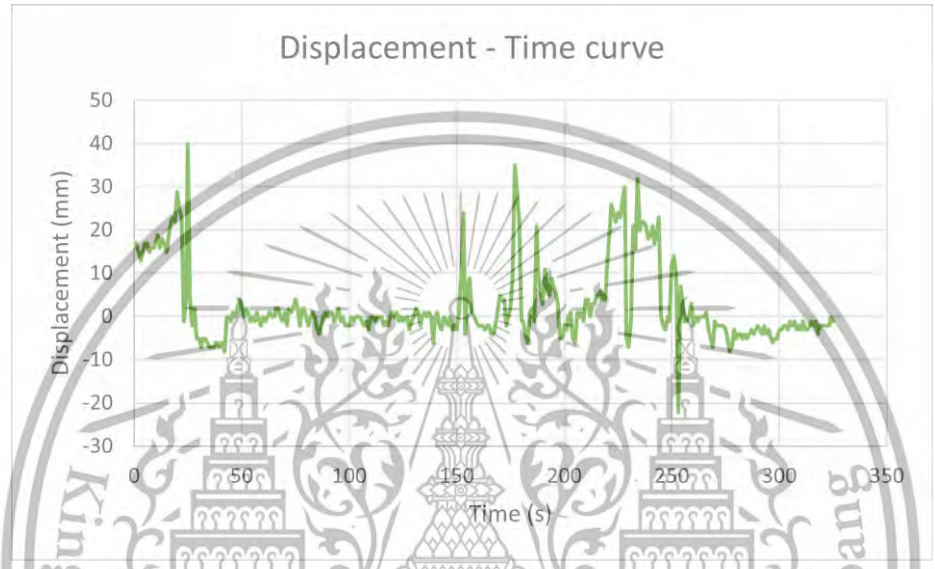

Figure 4.13 30% Displacement-Time Curve.

This graph shows the measure of deformation over time during the 30% strain. However, at a 30% strain level, the amount of generated stress exceeded the capacity, causing an overload which meant the motor was not able to compress the materials. Moreover, the data fluctuates more compared to the previous graphs due to the bending of the platform caused by the motor's inability to overcome the excessive force. The average output received is 2.560 mm which indicates that the machine was unable to determine the displacement under 30% strain condition.

4.3. Commercial Machine

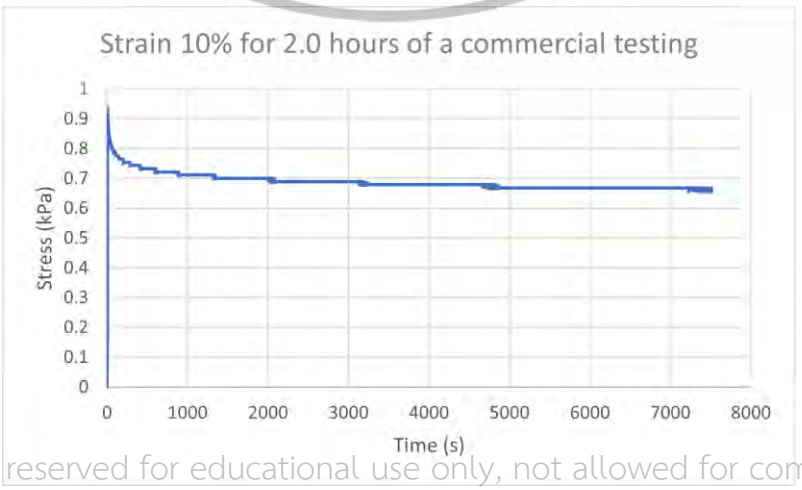

Figure 4.14 Strain 10% for 1.5 hours of commercial machine.

The graph obtained through testing using a commercial machine shows the theoretically expected stress relaxation characteristics. The maximum stress obtained in 10% strain was 0.937 kPa. In contrast, the graph generated by our assembled machine showed a maximum stress of 0.851 kPa as shown in (Figure 4.14). This indicates that our machine is capable of effectively demonstrating the viscoelastic properties of the material under stress. However, there are factors such as friction and shear stress, which can influence the materials response in multiple directions.

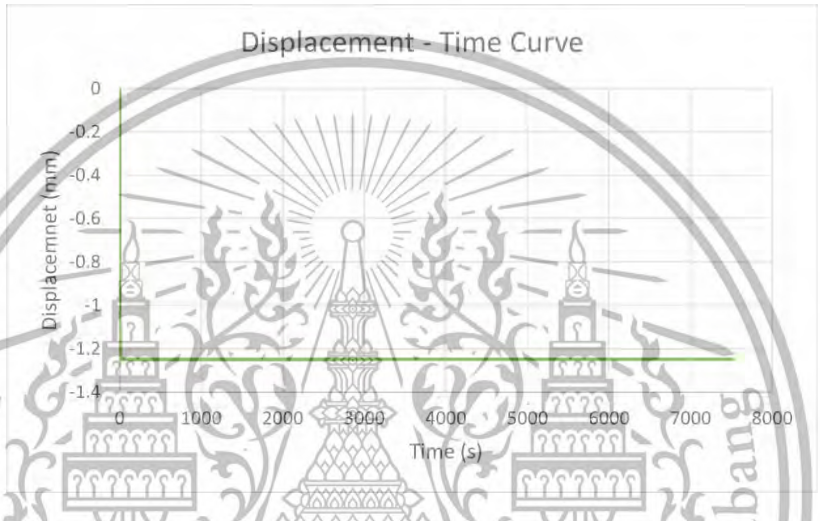

Figure 4.15 10% Displacement-Time Curve of commercial machine.

The displacement-time curve of a commercial machine demonstrates the theoretically ideal stress relaxation deformation graph. The average displacement obtained is -1.248 mm. However, the 10% assemble machine obtained -3.637 mm. This shows that the displacement of the assembly machine requires improvement due to the maximum stress obtained is close to the commercial machine's value. The assembly machine's sensor fluctuates at all times compared to the commercial machine which can affect the precision of the graph and data. Still, it is costly to get a high accuracy measurement displacement sensor at the laboratory scale.

CHAPTER 5
CONCLUSION

In this chapter, we begin by summarizing the capabilities of the load cell, stepper motor, displacement sensor, lead screw mechanism and other components in the context of in vitro viscoelastic testing machines. Next, we present several key conclusions based on the experiment conducted. Finally, we discuss our plans for future work and how we aim to ensure the machine's accuracy in laboratory scale.

5.1 Conclusions

In conclusion, the aim of this project was to characterize the viscoelastic properties of a material. We achieved this by designing and implementing a system consisting of a load cell, stepper motor, lead screw, displacement sensor, and a control system to generate a stress relaxation graph in each strain level (10%, 20%, 30%). The test in stress relaxation, our result graphs in each strain level similar to ideal theoretical graphs but depends on resolution of each component. The differences between our measurements and from a controlled laboratory setting can be attributed to several factors such as leadscrew accuracy, displacement sensor limitations, and the complexity of force application. These factors need to be considered for future adjustments of improving the accuracy and reliability of our stress measurements.

However, in Maxwell's model testing stress relaxation, we can detect the characteristic of viscoelastic properties of a material, the result graphs come out similar but not in the same trend as ideal theoretical graphs.

5.2 Future Work

We consider the performance and discuss errors in each component that the implementation has highlighted. While the results provide the material's behavior, It is important to acknowledge that errors in the assembly part, such as inaccurately in the force applied from the stepper motor or position of displacement sensor placed, may cause the inaccuracy of the results.

This suggests that it has the potential to be further developed into a device for characterizing viscoelastic properties when combined with a more effective displacement control system and careful calibration and we need to repeat the experiment to ensure our result. Additionally, mathematical equations can also be analyzed by fitting the obtained data.

REFERENCES

[1] Papanicolaou, G. C., & Zaoutsos, S. P., "Viscoelastic constitutive modeling of creep and stress relaxation in polymers and polymer matrix composites," in Creep and Fatigue in Polymer Matrix Composites (Second Edition), Woodhead, 2019, pp. 3-59

[2] Pruitt, L. A. and Chakravartula, A. M. Mechanics of Biomaterials: Fundamental Principles for Implant Design. Cambridge: Cambridge University Press, 2011

[3] Sukcharoen, K., Noraphaiphipaksa, N., Hasap, A. and Kanchanomai, C. "Experimental and Numerical Evaluations of Localized Stress Relaxation for Vulcanized Rubber," Polymers, vol. 14, no. 5, p. 873, Feb. 2022, doi: 10.3390/polym14050873

[4] Huang, D., Huang, Y., Xiao, Y., Yang, X., Lin, H., Feng, G., Zhu, X., Zhang, X,. "Viscoelasticity in natural tissues and engineered scaffolds for tissue," in Acta Biomaterialia, Elsevier Ltd, 2019, pp. 74-92.

[5] Yalcin, D., "Viscoelasticity Testing & Equipment," ADMET, [Online]. Available: https://www.admet.com/blog/viscoelasticity-testing-equipment/

[6] Kaur, K,. Gurnani, B., Viscoelastics. [Updated 2023 Jan 23]. In: StatPearls [Internet]. Treasure Island (FL): StatPearls Publishing; 2023 Jan-. from: https://www.ncbi.nlm.nih.gov/books/NBK578189/

[7] Mills, N., Jenkins, M., & Kukureka, S. (2020, 02 28). Plastics (Fourth Edition). Chapter 7 - Viscoelastic behaviour, 111-125. https://www.sciencedirect.com/science/article/abs/pii/B9780081024997000072

[8] Snoeijer, J. H., Pandey, A. K., Herrada, M. A., & Eggers, J. "The relationship between viscoelasticity and elasticity. Proc.R.Soc.A476: 20200419. p.2, 2020 https://doi.org/10.1098/rspa.2020.041

[9] Roylance D., "ENGINEERING VISCOELASTICITY," ENGINEERING VISCOELASTICITY, pp. 4-14, 2001.

[10] Doh, J., Kim, S.-W., & Lee, J. (2017). Reliability assessment on the degradation properties of polymers under operating temperature and vibration conditions. Proceedings of the Institution of Mechanical Engineers, Part D: Journal of Automobile Engineering, 095440701773526. doi:10.1177/0954407017735263

[11] Guedes, R. M., Creep and fatigue in polymer matrix composites, Cambridge: Woodhead, 2011..

[12] VISCOELASTICITY. (n.d.). https://www.uoanbar.edu.iq/eStoreImages/Bank/29.pdf

[13] "Force Sensor FSR402 Force Sensitive Resistor," CyberTice,[Online].Available:https://www.cybertice.com/product/1442/4-force-sensor-fsr402-force-sensitive-resistor-0g-10kg.

[14] "How to use a Load Cell (Strain gauge) using Arduino, HX711 and LCD Display," Youtube, 2021.

[15] "Load Cell Weight Sensor 200 Kg," CyberTice, 2021. [Online]. Available: https://www.cybertice.com/product/4534/load-cell-weight-sensor-100-kg-

[16] "TE Connectivity Vibration Sensor, 0°C → +70°C," RS-Online, [Online]. Available:https://th.rs-online.com/web/p/vibration-sensors/8937301+Vibration+Sensors-

[17] "Capacitive Force Sensor 8 mm 10 N (2.2 lbs)," Robotshop, [Online]. Available: https://www.robotshop.com/products/capacitive-force-sensor-8-mm-10-n-22-lbs.

[18] What is a force sensor, what are the different types of sensors and how do they work? (no date) FUTEK. Available at: https://www.futek.com/force-sensor.

[19] Interlink Electronics, Inc. FSR sensor, force sensing resistor, Interlink Electronics. Available at: https://www.interlinkelectronics.com/force-sensing-resistor

[20] Yaniger, S. I., "Force Sensing Resistors: A Review Of The Technology," Electro International, 1991, New York, NY, USA, 1991, pp. 666-668, doi: 10.1109/ELECTR.1991.718294.

[21] Kamble, V. A., Shinde, V. D. & Kittur, J. K. (2020). Overview of Load Cells. Journal of Mechanical and Mechanics Engineering, 6(3), 22–29.

[22] Regtien, P. and Dertien, E. (2018) Piezoelectric sensors, Sensors for Mechatronics (Second Edition). Available at: https://www.sciencedirect.com/science/article/abs/pii/B9780128138106000082

[23] Analog piezoelectric ceramic vibration module (no date) Cytron Technologies Thailand. Available at: https://th.cytron.io/p-analog-piezoelectric-ceramic-vibration-module

[24] Avnet. Inc, Capacitive pressure sensors, Pressure Sensors: The Design Engineer's Guide. Available at: https://www.avnet.com/wps/portal/abacus/solutions/technologies/sensors/pressure-sensors/core-technologies/capacitive/.

[25] Tobe, F. (2016). Capacitive sensors measure low forces, Design World. Available at: https://www.designworldonline.com/capacitive-sensors-measure-low-forces/

[26] "Telemecanique Sensors Diffuse Photoelectric Sensor, Miniature Sensor, 250 mm Detection Range," RS-Online, [Online]. Available: https://th.rs-online.com/web/p/photoelectric-sensors/2121804

[27] "Displacement Sensors CD22 series," [Online]. Available: http://www.jwtech.co.th/product/SENSOR/optex/CD22%20series.pdf.

[28] "Arduino GY-530 VL53L0X Laser ranging and gesture," CyberTice, [Online]. Available: https://www.cybertice.com/article/321/-arduino-gy-530-vl53l0x-laser-ranging-and-gesture.

[29] "Ultrasonic Distance Sensor (HC-SR04)," IOTCode, [Online]. Available: http://www.iot.codemobiles.com/product/5/ultrasonic-distance-sensor-hc-sr04.

[30] TOF050C VL6180 เซ็นเซอร์วัดระยะทางแสงเลเซอร์ ความแม่นยำสูง laser ranging sensor module ระยะตรวจจับ 0-50cm (no date) CyberTice. Available at: https://www.cybertice.com/product/4679/.

[31] Telemecanique sensors diffuse photoelectric sensor, miniature sensor, 250 mm detection range, RS. Available at: https://th.rs-online.com/web/p/photoelectric-sensors/2121804.

[32] Ultrasonic distance sensor (HC-SR04) - arduino.codemobiles.com, Code Mobiles. Available at: http://www.iot.codemobiles.com/product/5/ultrasonic-distance-sensor-hc-sr04.

[33] The Arduino, "What is Arduino Uno?," Arduino Documentation, https://docs.arduino.cc/learn/starting-guide/whats-arduino

[34] Ben, "What is an Arduino?," What is an Arduino? - SparkFun Learn, https://learn.sparkfun.com/tutorials/what-is-an-arduino/all

[35] "Choosing the right type of motor driver for your project," VLC Components s.l.,https://solectroshop.com/en/blog/choosing-the-right-type-of-motor-driver-for-your-project-n14#:~:text=A%20motor%20driver%20takes%20the,in%20the%20form%20of%20ICs

[36] "L298N motor driver module," Components101, https://components101.com/modules/l293n-motor-driver-module

[37] Olson, D., "All You Need to Know About Linear Stepper Motors, Their Actuators, and Their Applications," Venture Fgc, 06 2019. [Online]. Available: https://www.venturemfgco.com/blog/know-about-linear-stepper-motors-actuators-and-applications.

[38] "DC Gear Motor vs Stepper Gear Motor: All the differences," Micro Motors, https://www.micromotors.eu/en/dc-gear-motor-vs-stepper-gear-motor-all-the-differences/.

[39] Dejan, "How to Control Servo Motors with Arduino – Complete Guide," How To Mechatronics, [Online]. Available: https://howtomechatronics.com/how-it-works/how-servo-motors-work-how-to-control-servos-using-arduino/.

[40] "Basics of Air Pressure: Displacement Compression and Dynamic Compression," Atlas Copco, [Online]. Available: https://www.atlascopco.com/en-th/compressors/wiki/compressed-air-articles/displacement-and-dynamic-compression.

[41] "Hydraulic Press," Industrial Press, [Online]. Available: https://www.iqsdirectory.com/articles/hydraulic-press.html

[42] Aic, "AIC," AIC motor, https://aic.engineer/search-result/all/motor

[43] "Learn the basics of DC motors and small DC Gear Motors: ISL products," ISL Products International, https://islproducts.com/design-note/dc-motor-dc-gear-motor-basics/.

[44] Macfos, "Buy Planetary DC geared motor 350 rpm 78n-cm 24v IG45-14K online at robu.in," Robu.in | Indian Online Store | RC Hobby | Robotics, https://robu.in/product/planetary-dc-geared-motor-438-rpm-50-n-cm-24v-45mm/

[45] "Servo Motor Basics, working principle & interfacing with Arduino .," ElectronicWings, https://www.electronicwings.com/sensors-modules/servo-motor.

[46] "Linear Actuators 101 - everything you need to know about linear actuators," Firgelli Automations, https://www.firgelliauto.com/blogs/actuators/linear-actuators-101#:~:text=What%20is%20a%20Linear%20Actuator,simple%20push%20of%20a%20button.

[47] “12V micro linear actuator 50mm stroke 64N,” Cytron Technologies Thailand, https://th.cytron.io/c-dc-motor/p-12v-micro-linear-actuator-50mm-stroke-64n.

[48] “Hydraulic Press Machine Manufacturer,” Hydraulic Press Machine Manufacturer in India, https://lalithydraulics.com/hydraulic-press-machine-manufacturer.php

[49] The Arduino, “How to wire and program a button,” Arduino Documentation, https://docs.arduino.cc/built-in-examples/digital/Button.

[50] “6X6X1 push button 2 pins,” Cytron Technologies Thailand, https://th.cytron.io/p-6x6x1-push-button-2-pins.

[51] “Industrial Quick Search,” What Is It? How Is It Used? Types, Threads, https://www.iqsdirectory.com/articles/ball-screw/lead-screws.html.

[52] Sild, S., “Lead screws explained,” Fractory, https://fractory.com/lead-screws/

[53] Admin, “Screw pitch vs lead: What’s the difference: Blog posts,” OneMonroe, https://monroeengineering.com/blog/screw-pitch-vs-lead-whats-the-difference/#:~:text=Pitch%20is%20simply%20a%20measurement,are%20equal%20to%20each%20other

[54] Harvey Performance Company and Harvey Performance CompanyHarvey Performance Company’s team of engineers works together to ensure that your every machining challenge – from tool selection and application support to designing the perfect custom tool for your next job – is rectified with , “Multi-start thread reference guide - in the loupe - machinist blog,” Harvey Performance Company, https://www.harveyperformance.com/in-the-loupe/multi-start-thread-guide/

[55] “Single-start thread,” Single-start thread Per ASME B1.7-2006 Definitions, https://www.ring-plug-thread-gages.com/ASME-B1.7-Terms-Definitions/single-start%20thread.htm#:~:text=Single%2Dstart%20thread%3A%20the%20screw,useful%20for%20general%20fastening%20needs .

[56] Costen, E., “Screw thread types and their benefits,” Dimide, https://dimide.com/blogs/why-dimide/clamp-thread-types-their-benefits

[57] Gokilakrishnan, Divya, Rajesh, and Selvakumar, OPERATING TORQUE IN BALL VALVES-A REVIEW, vol. 2, no. 4, pp. 311–315, Dec. 2014.

[58] Singer, F. L., Engineering Mechanics: Statics and Dynamics. 3rd Ed. New York, etc.: Harper and Row, 1975.

[59] True, “Moment,” Trueplookpanya, https://www.trueplookpanya.com/learning/detail/33963

[60] Mathewbuer, “Stepper motor and L298N issues,” Arduino Forum, https://forum.arduino.cc/t/stepper-motor-and-l298n-issues/1039706

[61] “TOF050C VL618 Laser ranging sensor module Range 0-50cm,” CyberTice, https://www.cybertice.com/product/4679/tof050c-vl6180-

[62] Kanny, K., Mahfuz, H., Carlsson, L. A., Thomas, T., & Jeelani, S. (2002). Dynamic mechanical analyses and flexural fatigue of PVC foams. Composite Structures, 58(2), 175–183. doi:10.1016/s0263-8223(02)00160-5

[63] “สอนใช้งาน Arduino ทำเครื่องชั่งน้ำหนัก เซ็นเซอร์รับแรงกด วัดน้ำหนัก load cell HX711,” CyberTice, 2021. [Online]. Available: https://www.cybertice.com/article/312/สอนใช้งาน-arduino.

[47] “12V micro linear actuator 50mm stroke 64N,” Cytron Technologies Thailand, https://th.cytron.io/c-dc-motor/p-12v-micro-linear-actuator-50mm-stroke-64n.

[48] “Hydraulic Press Machine Manufacturer,” Hydraulic Press Machine Manufacturer in India, https://lalithydraulics.com/hydraulic-press-machine-manufacturer.php

[49] The Arduino, “How to wire and program a button,” Arduino Documentation, https://docs.arduino.cc/built-in-examples/digital/Button.

[50] “6X6X1 push button 2 pins,” Cytron Technologies Thailand, https://th.cytron.io/p-6x6x1-push-button-2-pins.

[51] “Industrial Quick Search,” What Is It? How Is It Used? Types, Threads, https://www.iqsdirectory.com/articles/ball-screw/lead-screws.html.

[52] Sild, S., “Lead screws explained,” Fractory, https://fractory.com/lead-screws/

[53] Admin, “Screw pitch vs lead: What’s the difference: Blog posts,” OneMonroe, https://monroeengineering.com/blog/screw-pitch-vs-lead-whats-the-difference/#:~:text=Pitch%20is%20simply%20a%20measurement,are%20equal%20to%20each%20other

[54] Harvey Performance Company and Harvey Performance CompanyHarvey Performance Company’s team of engineers works together to ensure that your every machining challenge – from tool selection and application support to designing the perfect custom tool for your next job – is rectified with , “Multi-start thread reference guide - in the loupe - machinist blog,” Harvey Performance Company, https://www.harveyperformance.com/in-the-loupe/multi-start-thread-guide/

[55] “Single-start thread,” Single-start thread Per ASME B1.7-2006 Definitions, https://www.ring-plug-thread-gages.com/ASME-B1.7-Terms-Definitions/single-start%20thread.htm#:~:text=Single%2Dstart%20thread%3A%20the%20screw,useful%20for%20general%20fastening%20needs .

[56] Costen, E., “Screw thread types and their benefits,” Dimide, https://dimide.com/blogs/why-dimide/clamp-thread-types-their-benefits

[57] Gokilakrishnan, Divya, Rajesh, and Selvakumar, OPERATING TORQUE IN BALL VALVES-A REVIEW, vol. 2, no. 4, pp. 311–315, Dec. 2014.

[58] Singer, F. L., Engineering Mechanics: Statics and Dynamics. 3rd Ed. New York, etc.: Harper and Row, 1975.

[59] True, “Moment,” Trueplookpanya, https://www.trueplookpanya.com/learning/detail/33963

[60] Mathewbuer, “Stepper motor and L298N issues,” Arduino Forum, https://forum.arduino.cc/t/stepper-motor-and-l298n-issues/1039706

[61] “TOF050C VL618 Laser ranging sensor module Range 0-50cm,” CyberTice, https://www.cybertice.com/product/4679/tof050c-vl6180-

[62] Kanny, K., Mahfuz, H., Carlsson, L. A., Thomas, T., & Jeelani, S. (2002). Dynamic mechanical analyses and flexural fatigue of PVC foams. Composite Structures, 58(2), 175–183. doi:10.1016/s0263-8223(02)00160-5

[63] “สอนใช้งาน Arduino ทำเครื่องชั่งน้ำหนัก เซ็นเซอร์รับแรงกด วัดน้ำหนัก load cell HX711,” CyberTice, 2021. [Online]. Available: https://www.cybertice.com/article/312/สอนใช้งาน-arduino.

[64] Das, S., How to Save Arduino Serial Data in TXT, CSV and Excel File. [Media]. Youtube. 2021